Applied Computer Science 2026, vol. 22, no. 1, pp. 1–19
https://doi.org/10.35784/acs_7413

Submitted: 2025-03-11 | Revised: 2025-09-25 | Accepted: 2025-09-30

Keywords: dead-reckoning sensor, optical mouse, azimuth sensor, gyroscope sensor, orientation

Toshihiro YUKAWA [1*]
[1] Iwate University, Japan, yukawat@iwate-u.ac.jpt
[*] Corresponding author: yukawat@iwate-u.ac.jpt

Development of a dead-reckoning sensor system for indoor environments

Abstract

This paper presents a method for constructing a dead-reckoning sensor system for indoor environments that enables autonomous control of a mobile robot. The proposed technique includes a method for achieving accurate autonomous control of robots. Using existing electronic equipment, we propose a system to measure the actual position and azimuth of mobile robots. The synthesis of information from sensor data into time series data of actual transition movement record of the mobile robot, and the algorithm of programming installed in a microcomputer and a PC for controlling peripheral devices around sensors influences the accuracy in estimating its position/posture. The dynamic characteristics of the mobile robot can be derived using induction theory for the system that installs a mouse device. The objective of the study for the mobile robot corresponds to a novel autonomous robot as an assistant without any guideline or other induction by GPS indoors. Here we discuss the adequacy of the sensor system that determines the positional accuracy of the robot. The position and orientation of the robot can be determined using a gyroscope and azimuth sensors. Finally, we investigate the performance of the robot indicated by the sensor system for a dead-reckoning strategy with optical sensors, orientation sensors, and gyroscope sensors to achieve highly accurate self-position estimation for a mobile robot moving indoors in the experiment.

1. INTRODUCTION

Sometimes, in confined indoor environments, autonomous mobile robots may collide with obstacles or become stuck. From a mechanical point of view, the robot should have an omnidirectional motion mechanism. In addition, from a control point of view, robots need technology to estimate their precise position and direction. Mobile robots equipped with omnidirectional wheels have high performance in omnidirectional motion. However, even with this mobile robot, it is difficult to achieve precise self-position estimation with high accuracy when the wheels installed in the robot slip. When considering the realization of self-position estimation of a robot using GPS, a new problem with GPS arises. To receive GPS radio waves over large areas indoors, an additional communication base is needed.

In this paper, we focus on an optical mouse and develop a new estimation system for the self-position and direction of a robot. An optical mouse is originally a device that allows a mouse cursor to be moved on a monitor. By equipping the robot with the optical mouse sensor, we try to measure the two-dimensional movement of the robot. Most optical mice can measure the two-dimensional movement of the main body of the mouse in the local coordinate system, but they cannot measure the direction of the mouse itself. Therefore, we use additional gyroscope sensors to detect changes in the direction of the mouse mounted on the robot. The rotation angle of the mobile robot, which can be estimated using an orientation sensor such as a gyroscope sensor, provides information about its position and direction. Therefore, we develop a sensor system that combines an optical sensor, an orientation sensor, and a gyroscope sensor. The proposed dead-reckoning navigation system provides highly accurate self-position estimation even when the wheels of a mobile robot slip on the floor indoors, where GPS radio waves cannot reach.

2. HISTORICAL BACKGROUND

In the past, there have been many studies on the guidance and control of various types of robots. The book by Nikolaus Correll et al. (2021) is written about the importance of mapping, which is the process of building representations of the environment, and path planning, which allows autonomous mobile robots to find a path to move between two points. Mapping information for automation and path planning is critical for operating mobile robots in real environments to provide them with information about the surfaces and obstacles. For various optimizations, such as minimizing path length, minimizing acceleration/deceleration, and minimizing number of turns, the choice of planning algorithm must satisfy several evaluation criteria. Saddek Bensalem et al. show that it is possible to use structural analysis techniques for deadlock detection and safety property verification (2009). By using online monitoring of execution at the functional level with observer components, feedback actions can be generated for the decision level, which is appropriate for error recovery. They have also fully implemented a GenoM/BIP controller for the navigation part of a functional layer of DALA (an iRobot ATRV), running in simulation and on the real robot. The controller is enforced online by the construction of the interaction model. To extend the BIP model to consider the decision capabilities of autonomous robots, they were able to construct a model of the decision layer and components. In the book by Lewis and Ge (2006), efforts in the study and development of visual guidance technology for autonomous vehicles were explained in two major categories, such as unmanned ground vehicles (UGVs) and intelligent transportation systems (ITSs). The focus was on visual guidance and how it defines the following roles of vision systems: detecting and following a road, detecting obstacles, detecting and tracking other vehicles, and detecting and identifying landmarks. Since robots are required to navigate in crowded environments, Noriaki Imaoka et al. (2020) have proposed a new method of autonomous movement that is compatible with the physical contact signalling used by humans. They have proposed a novel method for navigating through a human crowd using a conventional autonomous mobile robot drive system and an involute-shaped hand with a one-DoF arm, and the effectiveness of the technique has finally been experimentally confirmed. Yusuke Tsunoda et al. (2023) constructed a shepherding robot system using diffraction in the interaction between sound and obstacles to verify the shepherding robot navigation system in an environment with obstacles. They also applied their proposed shepherding model to a mobile robot using a sound source direction estimation method and distance determination. Guidance experiments confirmed the practicality of the proposed system and verified its validity. DeSouza et al. (2002) reviewed various aspects of the progress made in vision for mobile robot navigation. They found that, compared to twenty years ago, there is a much better understanding of the problems faced by developers trying to equip mobile robots with sensory intelligence, and that the different representation schemes vary in the degree of metric knowledge they contain, exhibit different degrees of robustness to illumination variations, etc. Morales et al. (2009) described a self-contained mobile robot for autonomous navigation in outdoor pedestrian walkways. They also reported on the difficulties of navigation in outdoor walkways, mostly covered by trees, and their system integration approach. For localization, a multi-sensor approach was implemented using an EKF for data fusion of wheel encoder, IMU, GPS, and laser scanner sensors. In addition, an effective method for detecting roads with significant amounts of fallen leaves was proposed. Ichihara et al. (2022) developed the guide robot and achieved human-tracking navigation without changing the configuration of the navigation system, by which the robot navigated autonomously along a preset route in the museum. They also demonstrated that two types of guidance services can be provided based on the visitor's request by seamlessly switching between the autonomous navigation method and the human-tracking navigation. In addition, they conducted an experiment to verify the system at the Muffler Museum, where the guide robot successfully navigated in two modes with a human visitor. Kidono et al. (2000) proposed a navigation method of a mobile robot based on the map autonomously generated by the robot. While the robot is moved by the human guide, the robot makes the map, which includes object boundaries, by integrating the observed object points. After making the map, the robot detects the shortest path and plans to view directions from each viewpoint. The robot can reach the destination safely and efficiently by using the plan. Kaito Ichihara et al. (2022) developed the guide robot and achieved human-tracking navigation without changing the configuration of the navigation system, by which the robot navigated autonomously along a preset route in the museum. They demonstrated that two types of guidance services can be provided based on visitor requests by seamlessly switching between the autonomous navigation method and human tracking navigation. They also conducted an experiment to verify the system at the Muffler Museum, where the guide robot successfully navigated in two modes with a human visitor. Kidono et al. (2000) proposed a navigation method of a mobile robot based on the map autonomously generated by the robot. While the robot is moved by the human guide, the robot makes the map, which includes object boundaries, by integrating the observed object points. After making the map, the robot determines the shortest path and plans to view directions from each viewpoint. Using the plan, the robot can reach the goal safely and efficiently. Boris Sofman et al. (2006) have proposed a self-supervised online learning algorithm and shown how the algorithm can improve the navigation capabilities of unmanned ground vehicles by learning in real time to interpret overhead and remote sensor data to predict terrain traversal costs generated by an on-board perception system. They demonstrated the proposed approach through field tests aboard a large robot in complex natural environments. The algorithm significantly improved the quality of the robot's navigation performance. Kuanqi Cai et al. (2023) have noted that their experiments demonstrate the effectiveness of their proposed approach over several baseline methods for robot navigation. Their method ensures human comfort while reducing collision risk. Their proposed curiosity-based method achieves a human-friendly path by taking into account the localization uncertainty of the robot and the distribution of the crowd. Experiments on various scenarios show that the method performs well in large and crowded environments. Bu et al. (2023) have proposed a detection framework for mobile robot navigation based on computer vision and deep learning. Their study aims to automatically navigate the mobile robot in complex traffic situations by deliberately combining several algorithms and the YOLOv5 model. Their proposed framework not only ensures obstacle avoidance, but also stabilizes the robot at its desired position and orientation despite slippage. Czarnecka et al. (2018) presented an algorithm for programming the end-effector path of an industrial robot based on 2D images. They have also given a brief overview of modern solutions for the implementation of industrial robots. They have described the test setup and the software used in the tests. Furthermore, they have presented the key elements of the controller algorithm and its operation as 2D image processing with MATLAB software, generation of robot control codes in AS language, and implementation of the generated codes on the Kawasaki RS003N robot (Czarnecka et al., 2018). As a study of autonomous vehicle motion, a taxonomy of on-road driving behaviors has been analyzed to produce sets of specifications that identify the world model entities, features, attributes, resolutions, detection distances, and locations for each individual driving task (Barbera et al., 2003). With respect to a ground contact sensor to complement the dead reckoning sensor, as an evolution of the original and unique sensor, a compliant tactile sensor made of silicone rubber with a spherical shell geometry has been studied experimentally and numerically. Their bio-inspired sensor has characteristics critical for robotic applications and has been tested in actual robots performing sensitive manipulation. The sensor has properties that allow the estimation of both normal and shear contact forces independent of the object geometry (Sina Youssefian et al., 2014). For the sensor integration system, an integrated proximity, contact, and force sensor has been presented. The proposed sensor has a wide range of use cases that facilitate grasping and manipulation, ranging from contact point detection and grasp point determination to object registration (Patel et al., 2018).

3. SELF-LOCATION ESTIMATION METHOD IN INDOOR

As mentioned above, some researchers have studied and focused on autonomous movement methods and self-location estimation for autonomous mobile robots to navigate safely indoors. To achieve highly accurate autonomous motion and self-location estimation indoors, it is necessary to solve problems that do not exist in autonomous motion outdoors. One of the problems to be solved is the inability to receive GPS signals. Although GPS is generally used for autonomous outdoor movement, since there are many roofs and obstructions indoors, a method that does not use GPS is needed. There is a high probability that the space in which a robot can move indoors is limited, especially in a house that is narrow and filled with obstacles.

Figure 1(a) shows the interior walls, doors, and obstacles of a typical home. When a robot moves, it must avoid colliding with obstacles. Of course, a basic requirement is that the robot must be able to move accurately. To solve these problems, the robot should have an omnidirectional mobile mechanism that excels in fine motion.

A conceptual diagram of the movement of a mobile robot with an omni-wheel, which is a type of omnidirectional mobile mechanism, is shown in Figure 1(b). Its basic motion patterns are straight motion, traversing, turning, and rotating. Omni-wheels are capable of translational and rotational movements in any direction without turning back, and their usefulness has attracted attention.

We design a mobile robot with omni-wheels that moves by causing active slippage between the omni-wheel surface and the ground while measuring the distance travelled using an encoder count. Even if the rotation amount is measured by directly applying the rotation axis of the encoder to the floor, there is a high possibility of error due to slippage (Figure 2(a)).

Therefore, we focused on the optical sensor mounted on an optical mouse. The sensor used in an optical mouse is originally mounted to enable pointing with the mouse cursor. By controlling the optical sensor mounted on an optical mouse, it is possible to obtain two-dimensional position information of the robot's movement without affecting the situation of its wheel deformation or slippage.

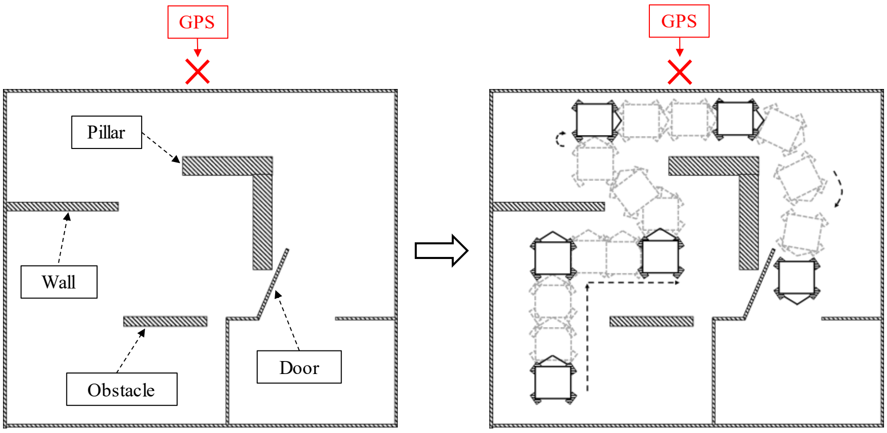

(a) Indoor structure and environment (b) The movement patterns of the robot

Fig. 1. The mobile robot in an indoor environment

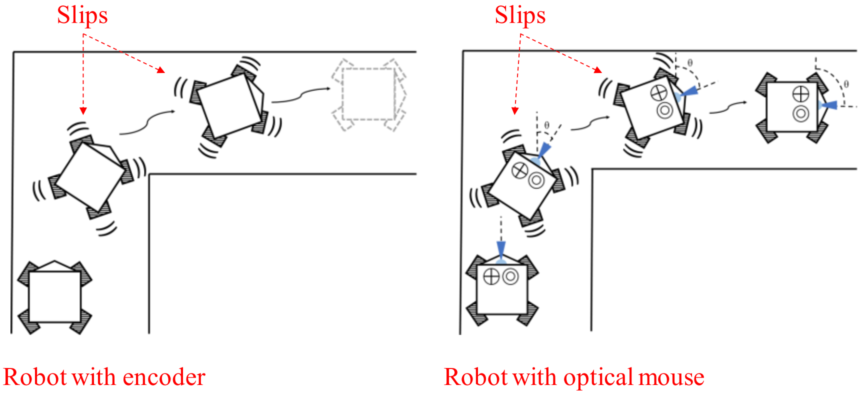

(a) The robot with only encoders (b) The robot equipped with various sensors

Fig. 2. The mobile robot, which moves through the corridor

When trying to obtain the amount of movement using an optical sensor, the problem is detecting the direction of the robot. Although the optical sensor in an optical mouse is a product designed to measure movement in two dimensions, it cannot detect rotation or changes in the direction of the optical sensor itself. Therefore, we focused on a direction sensor that detects geomagnetism, and obtained information about the robot's attitude using a direction sensor that reads geomagnetism. In addition, to avoid the influence of the direction sensor error on the measured value, we try to reduce the error of the direction sensor by using an additional gyro sensor to detect the occurrence of angular velocity (Figure 2(b) shows an image of the mobile robot with various sensors, such as an optical sensor, a direction sensor, and a gyro sensor).

Thus, by combining an optical sensor, a direction sensor, and a gyro sensor, we develop a sensor system that can accurately obtain data on the amount of movement and attitude of the aircraft, even if the wheels slip, even in indoor locations where GPS signals cannot reach.

4. MOBILE ROBOT

First, we explain the mobile robot equipped with the proposed sensor system. The omni-wheeled robot, manufactured by Tosa Denshi Co., Ltd., is used as the base for the mobile robot. The size of the mobile robot is 220 mm in length, 220 mm in width, and 100 mm in height, and it has omni wheels, which can be an omnidirectional moving mechanism. The robot is a mobile robot with four pairs of omni-wheels. Each motor controls each omnidirectional wheel independently. The omnidirectional wheel installed in the robot can also be operated manually by the operator using the VS-C3 robot dedicated controller manufactured by Vstone Co., Ltd.

Figure 3 shows the appearance of the omni wheel robot equipped with the sensor developed in this paper. A tablet PC, WN891, manufactured by Mouse Computer Co., Ltd., is used to display and store output data from the various sensors. To set a tablet PC on the omni-robot, a thin plate housing is mounted, and the control board and sensor board are on the plate. Figure 3(a) shows the omni-robot with the sensor board and tablet PC mounted, and Figure 3(b) shows the exterior (rear) of the robot with the components for mounting an optical mouse and the board for controlling the optical mouse attached.

5. SENSOR

5.1. Optical sensor

The dead-reckoning method is one of the methods of estimating the position of the mobile robot by accumulating information on the amount of movement obtained from sensors mounted on the robot's body. Here, we explain a dead-reckoning method using optical, orientation, and gyroscope sensors. As mentioned above, Figure 3(a) shows a robot moving down a corridor with its wheels sliding, and Figure 3(b) shows the movement image of the robot with the optical mouse. An optical mouse equipped with an optical sensor captures the image reflected on the lens in real time and compares it with past image data to calculate the amount of movement of the mouse body. The coordinate data, divided into x-y coordinates in the local coordinate system of the sensor, is output to the motherboard in the PC main body through the dedicated mouse cable. A wired blue LED mouse (MA-BL2UPS, manufactured by Sanwa Supply Co., Ltd.) controlled by a PIC microcontroller (PIC16F886, manufactured by Microchip Technology Co., Ltd.) obtains the amount of movement in two dimensions. The interface for communication between the sensor and the PIC microcontroller complies with the PS/2 standard.

Figure 4(a) shows the structure of an optical mouse consisting of main parts such as a light source, prism, optical sensor, and integrated circuit board. In the dead-reckoning of the robot indoors, as the structure and material of the floor change depending on the indoor environment or buildings, the sensor system must be able to operate on all kinds of materials or design patterns on the floor. To accommodate this situation, a blue light LED, such as a light source, is mounted on the optical mouse system. Generally, among optical mice, the mouse that can read the most diverse surfaces uses blue LEDs. It is possible to read the irregularities on the reading surface with higher accuracy using the blue light LED, whose wavelength is shorter than that of red light. The blue LED can measure the movement of the robot on even, glossy surfaces, cloth surfaces, and opaque glass surfaces. The operating parts, such as the cover and buttons mounted on the optical mouse, as well as the several parts connected to the electronic board, are removed. We use the mouse device without these removed parts in the sensor system. Figure 4(b) shows the electric board of the mouse device without the removed parts in the sensor system after the operating parts, such as the cover and buttons mounted on the optical mouse, as well as several parts connected to the electronic board, are removed.

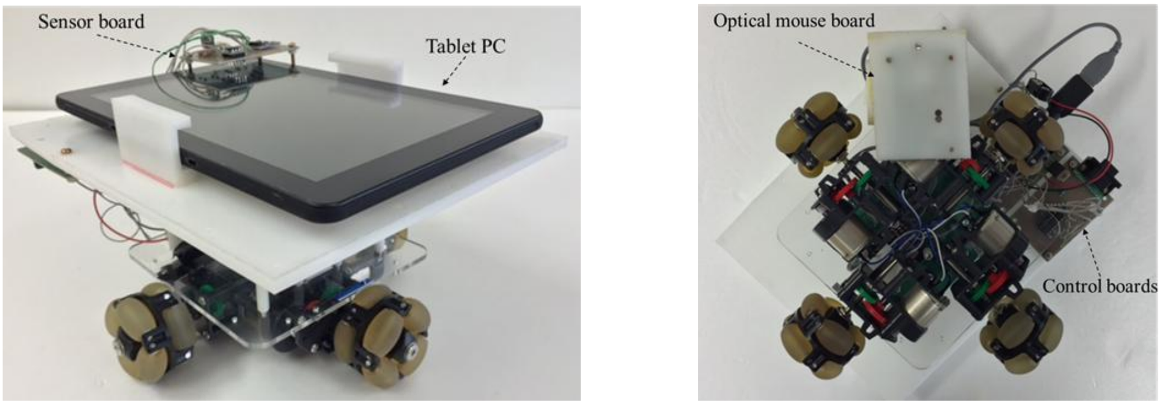

(a) The mobile robot with the PAsensor system and tablet PC

(b) The mobile robot with the optical mouse board and the control boards (backside)

Fig. 3. The mobile robot with the control system and tablet PC

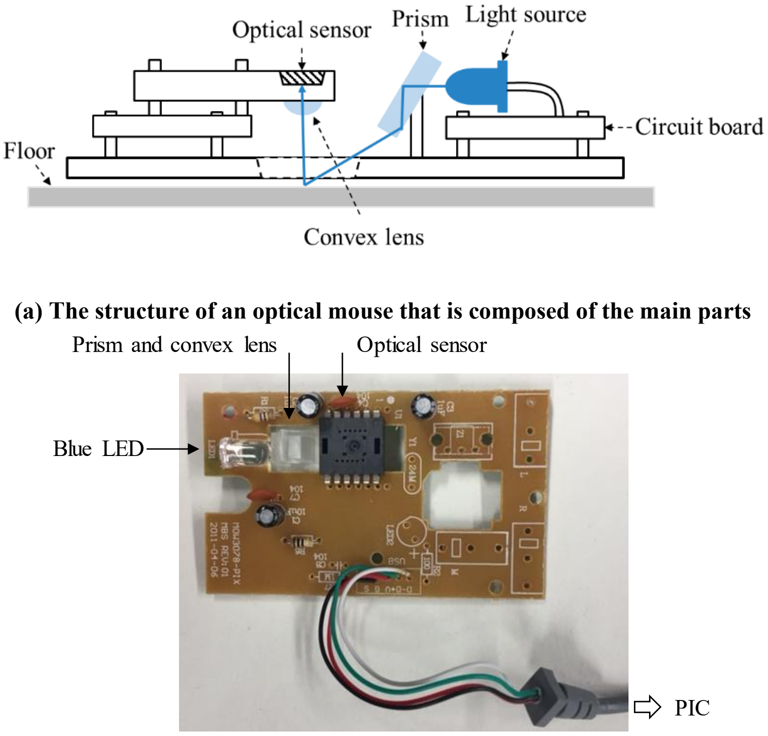

(a) The structure of an optical mouse that is composed of the main parts

(b) The circuit board in an optical mouse

Fig. 4. The structure of the circuit board installed in the optical sensor

5.2. Orientation sensor

The orientation sensor is used to detect direction data. The orientation sensor using geomagnetism measures the direction of the vehicle or mobile robot, etc. It captures the direction data as angle data for the robot's coordinate guidance and detects changes in the robot's posture. A digital compass module (HMC6352, manufactured by Honeywell Co. Ltd.) obtains changes in the posture of a mobile robot as angle data by using Honeywell's 2-axis digital compass module HMC6352. Table 1 lists the specifications of the HMC6352. Figure 5 shows the sensor module itself and its internal schematic. Figures 6(a) and (b) show photos of the sensor (front and back).

The HMC6352 orientation sensor, along with other orientation sensors, detects magnetic north and returns data centered on accurate magnetic north. Magnetic north is only the orientation of north that a compass points to, and it is known to deviate by several degrees from the true geographic north of the Earth (the North Pole). The deviation depends on the location on the Earth. The difference between true north and magnetic north is called magnetic declination, and it changes depending on the location on the Earth and the time. The declination in the city where we live is about 8 degrees. Since the purpose of the study is to measure basic data on the posture of a mobile robot, we do not take declination into account. The HMC6352 orientation sensor indicates North as 0°, East as 90°, South as 180°, and West as 270°.

Tab. 1. Specifications of the azimuth sensor

Supply voltage	2.7~5.0 V
Heading resolution	1.0°
Detection range	0~3599
Operating temperature	-20~70°C
Interface	I^2C
Weight	0.14 g

The HMC6352 orientation sensor has a resolution of 0.1°. The values returned by the sensor are numbers between 0 and 3599. The HMC6352 orientation sensor uses an I2C interface. I2C communication is a two-wire serial communication system consisting of a data line (SDA) and a clock line (SCL). The PIC16F886 microcomputer is connected as the master device, while the HMC6352 orientation sensor is connected as the slave device in I2C communication. The slave address of the HMC6352 is 0x42. In I2C communication, the master sends instructions to the slave address 0x42 to receive the required data. Figure 7 shows an example of I2C communication.

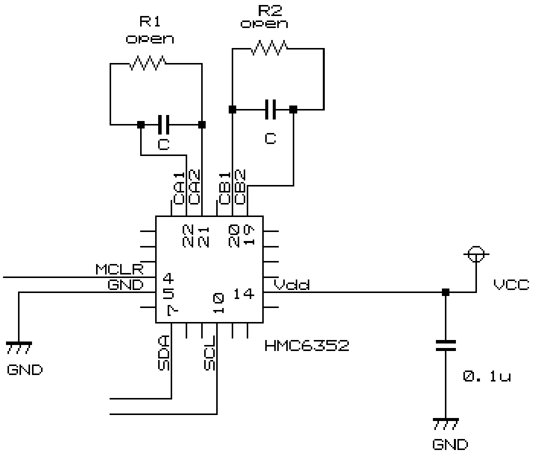

Fig. 5. Internal circuit of the azimuth sensor

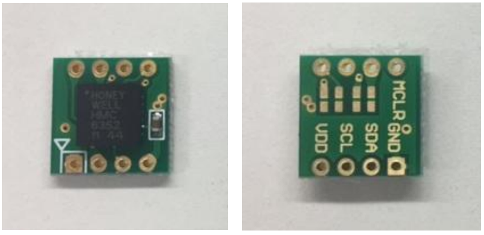

(a) Front side **(b) Back side**

Fig. 6. Azimuth sensor HMC6352r

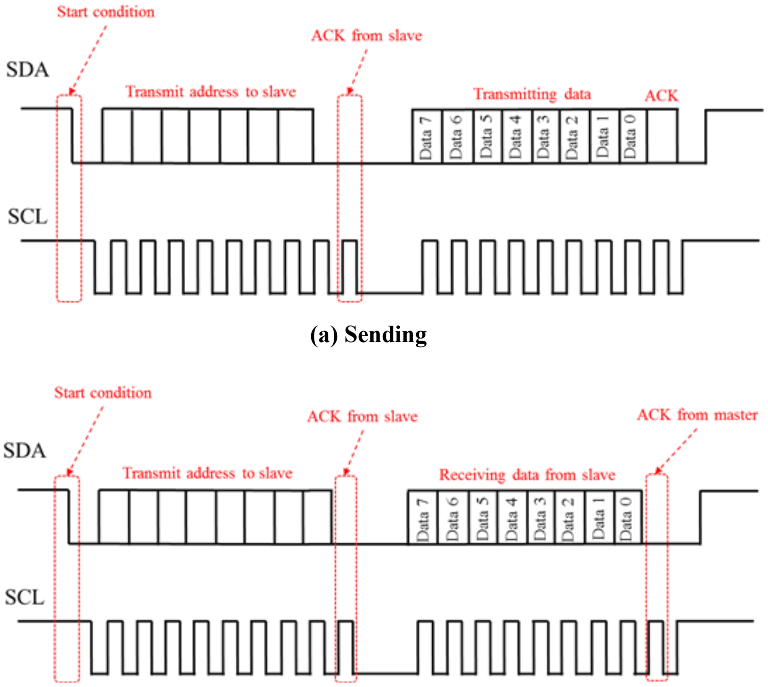

(a) Sending

(b) Receiving

Fig. 7. I^{2}C master mode waveform

5.3. Gyroscope sensor

Gyroscope sensors can detect the angular velocity of the sensor body, and it is possible to determine the rotation angle of the sensor itself through time-integration processing by the microcomputer. Some measurement errors occur in the gyroscope sensor due to temperature changes and electrical noise in the environment where the sensor is mounted. The measurement errors accumulate during the integration process.

We select a sensor module equipped with a piezoelectric vibration gyroscope (ENC-03R manufactured by Murata Manufacturing Co., Ltd.) in the system. The vibration gyroscope vibrates the internal element, detects the Coriolis force acting on the internal element as it rotates, and calculates the angular velocity. Coriolis force is a type of inertial force that acts in a rotating coordinate system. The gyro module is used to detect camera shake and vibration in vibration-proof devices. However, it is not suitable for calculating the rotation angle of a mobile robot or the like.

To estimate the offset error, other methods have been developed that combine the gyro sensor with odometry using wheel encoders or an algorithm, and correct the detection error in a controller or program. These are often used to control the posture of a mobile robot. In the gyro sensor module, a built-in circuit eliminates drift and electrical noise due to temperature changes. However, due to the effects of errors in the circuit mentioned above, it is difficult to output the correct angular velocity. Therefore, the best way to use the sensor module is to detect rotation and vibration. Although the gyro module is the product that detects the rotation of a mobile robot, it is only used to prevent detection errors or malfunctions in the HMC6352 orientation sensor from being added to the data on the robot's rotation angle in this paper. Thus, the gyroscope module is only used to detect changes in the orientation of the mobile robot. Figure 8 shows the internal processing flow of the ENC-03R gyro module, Figure 9 shows the internal circuit diagram of the gyro module, Table2shows the specifications of the gyro module, and Figure 10(a) and (b) show the photographs (front and back) of the gyro module.

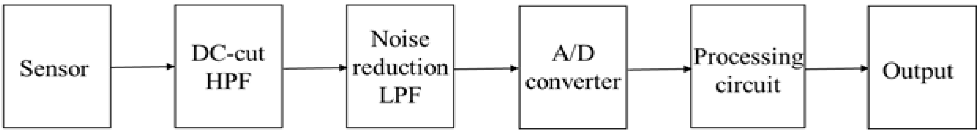

Fig. 8. Flow chart of the gyroscope sensor

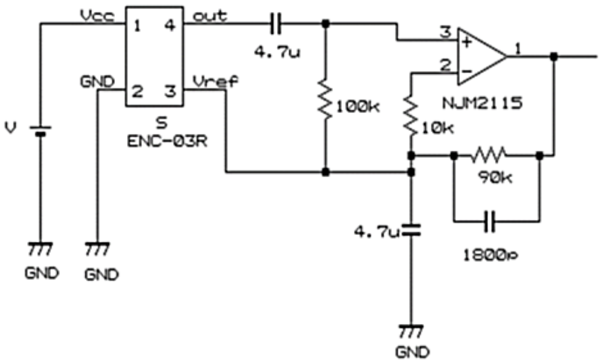

Fig. 9. Internal circuit of the gyro module sensor

Tab. 2. Specification of gyro module sensor

Supply voltage	2.70~5.25 V
Detection range	-300 ± 300°
Sensitivity	0.67 mV/deg/s
Linearity	±5 %FS
Operation temperature	-5 ± 75°C

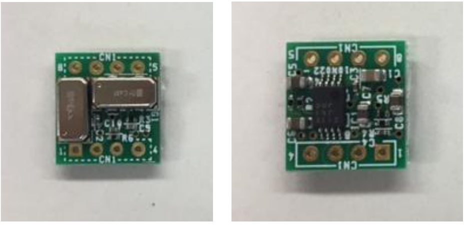

(a) Front **(b) Back side**

Fig. 10. Gyro module ENC-03R

6. PA SENSOR SYSTEM

6.1. Assembly development of the PA sensor system

In this paper, we define the sensor system combining the position and azimuth sensor with the optical mouse sensor, orientation sensor, and gyroscope sensor module as the PA sensor system (Position and Azimuth Sensor System). A PIC microcontroller, PIC16F886, controls the PA sensor system. The data obtained from the PA sensor system is output to the Tablet PC via RS-232C standard serial communication. The communication speed is 9600 bps. The PIC microcontroller, PIC16F886, and the PC can communicate via an Intersil Americas Inc. transceiver IC, ICL3232CPZ. Figure 11 shows the block diagram of the PA sensor system.

6.2. System circuit design

Figure 12 shows the functions of each pin of the PIC16F886 when designing the sensor system circuit in this study. Figure 13 shows the schematic developed. The power supply voltage is regulated to 5 V by the STMicroelectronics L7805CV-DG three-terminal regulator.

In addition to the orientation sensor module, HMC6352, a three-axis geomagnetic sensor, we installed another sensor module, HMC5883L,manufactured by Parallax Inc. as a spare orientation sensor module. The interface of the HMC5883L is I2C, just like the HMC6352.

6.3. Position and orientation detection algorithm

We describe the algorithm for detecting the position/orientation of the mobile robot. First, the gyro module sensor installed on the robot detects the angular velocity of the base. After the main power is turned on, the output value of the gyro module sensor is measured 100 times with a sampling period of 0.1 s while the robot is stationary. Then, the average value of these data output from the sensor is calculated, and this average value is set as the initial angle. The difference value of the angle data in each time series is derived from the time difference between the angle value obtained in each sampling period and the initial difference value, and is calculated as the approximate angular velocity obtained by the Euler approximation. Similarly, after power on, the output value of the orientation sensor is measured 10 times with a sampling period of 0.15 s while the robot is stationary. This average value is the initial orientation, and the difference between the orientation value obtained at each sampling period and the initial orientation is the rotation angle of the mobile robot. Next, the program measures the amount of movement is executed. First, the optical mouse on the robot measures the x-y amount of movement in the local coordinate system of the mouse itself. The gyro sensor then determines whether the body is rotating or not. If it determines that it is not rotating, the optical mouse value is output to the PC as the robot's amount of movement. If it determines that it has rotated, the coordinate conversion is performed using the following equation (1).

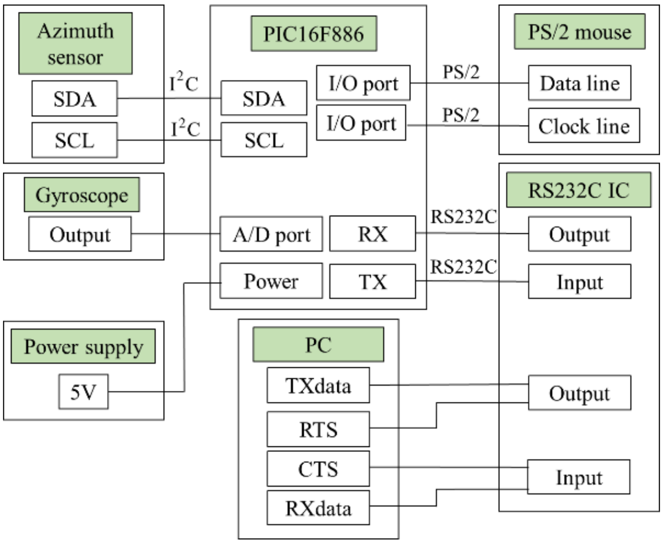

Fig. 11. The configuration of the PA sensor system

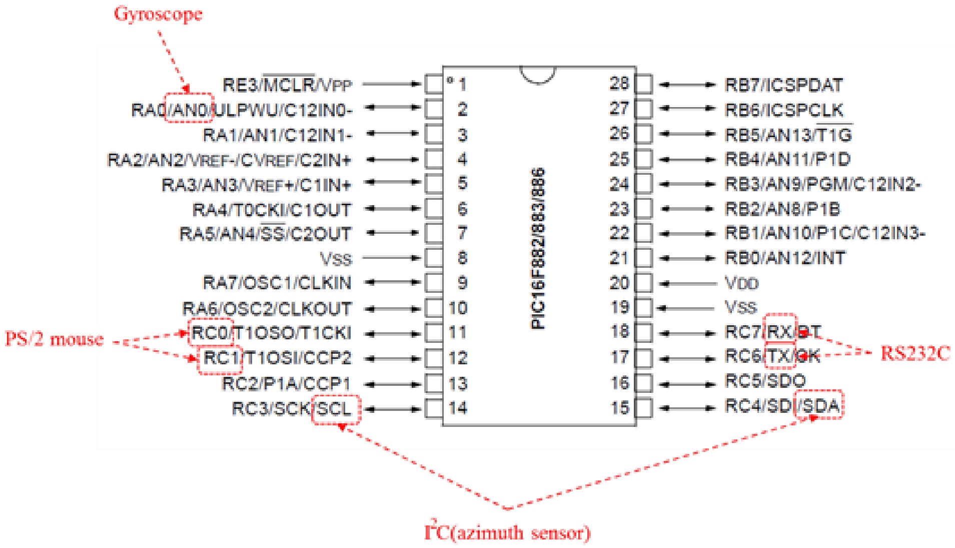

Fig. 12. Pin assignment of PIC16f886

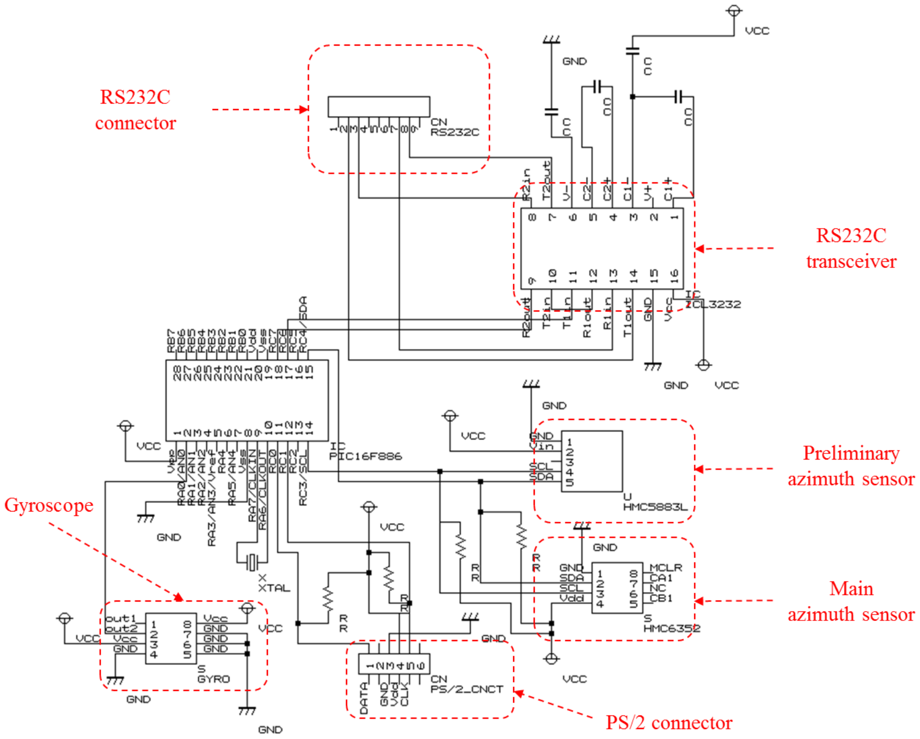

Fig. 13. Circuit diagram of the PA sensor system

$$\begin{bmatrix} x' \\ y' \end{bmatrix} = \begin{bmatrix} \cos\theta & -\sin\theta \\ \sin\theta & \cos\theta \end{bmatrix} \begin{bmatrix} x \\ y \end{bmatrix} \tag{1}$$

The values of X and Y are output to the PC as the amount of movement of the robot by the algorithm using equations (2) and (3).

$$X = \sum_{i=0}^{\infty}(x_i \cos\theta_i - y_i \sin\theta_i) \tag{2}$$

$$Y = \sum_{i=0}^{\infty}(x_i \sin\theta_i + y_i \cos\theta_i) \tag{3}$$

The measurement program continues as a continuous loop unless an exit instruction is executed. Figure 14 shows a block diagram of the PA Sensor System at this point, and Figure 15 shows a flowchart of the PA Sensor System program.

6.4. Design of electronic boards for measurement systems

Based on the circuit and algorithm designed in the previous section, we have made both software programs and an electronic board for installation in the mobile robot. The size of the boards is 46 mm x 70 mm. A total of three boards are combined. Using high-heat dissipation single-sided copper-clad boards manufactured by Yajima Manufacturing Co., Ltd., we processed a special board with an i-model IM-01 manufactured by Roland DG. After removing the peripheral components from the board installed in an optical mouse, we reused the special board for the optical sensor. Figure 16 shows the finished board.

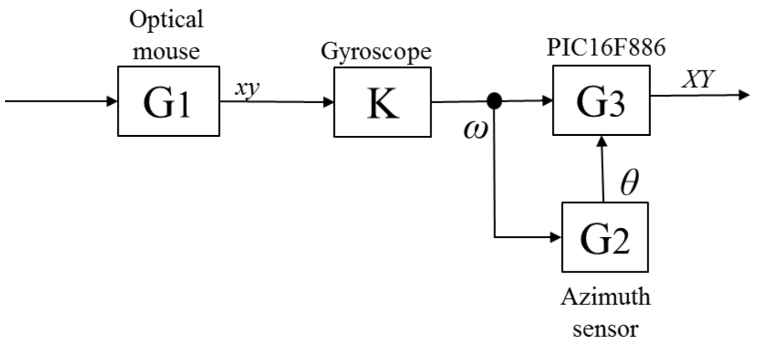

Fig. 14. Block diagram of the PAsensor system

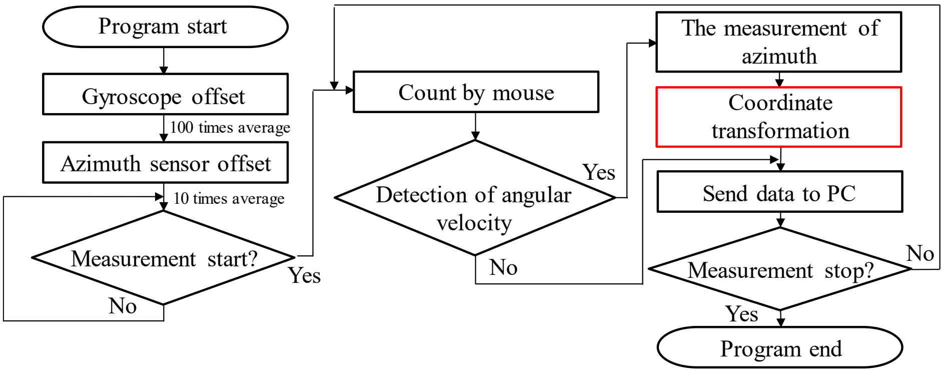

Fig. 15. Flow chart of the PA sensor system

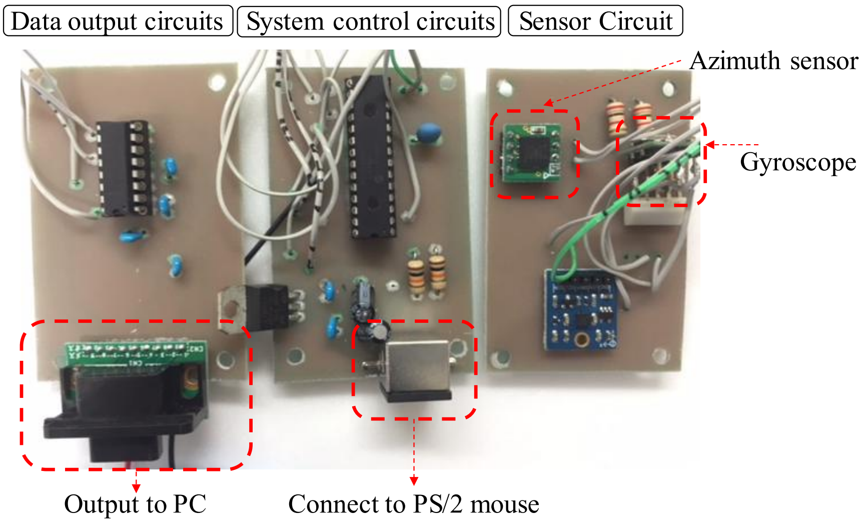

Fig. 16. Electronic boards of the PA sensor system

6.5. PS/2 Interface connector

We programmed it with special software to control the PS/2 interface with a PIC microcontroller. There are two types of PS/2 interface connectors:5-pinand 6-pin. The optical mouse used in this study has a 6-pin connector. The mini-DIN connector connects to the PIC16F886. Figure17shows the pinout of the PS/2 connector. Out of a total of six pins, four pairs of pins are used to control the interface, i.e. pins 1, 3, 4, and 5. Pin #1 is for the data line. Pins that are input to or output from the mouse are used for these pins, and the data of the mobile robot's movement amount is output through the pins. Pin #5 is for the clock line. The mouse connected to the PS/2 interface outputs a clock signal through these pins and monitors the signal. Communication with the host PIC16F886 was performed in real time by inputting the mouse clock to pin #1 and simultaneously outputting data from the pin.

We can set the clock time in the PS/2 mouse control system to any value in the range from a minimum of 60 µs to a maximum of 100 µs. We also select the mouse movement speed to be any value lower than the sampling interval time during the calculation in the PIC microcontroller. Pins 3 and 4 are for connection to ground and power, respectively. The supply voltage range for the PS/2 interface was 4.5 to 5.5 V, and the maximum supply current was 275 mA. Both data and clock lines were connected to pull-up resistors of 1 to 10 kΩ.

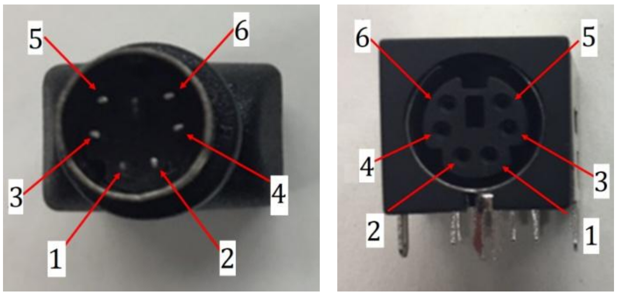

(a) Plug **(b) Socket**

Fig. 17. The PS/2 connector pin assignments

Tab. 3. Basic rules for communication with the PS/2 interface

PS/2 bus states	Data line	Clock line	Control state
Immediately after power-on	High	High	Idle state
When controlling I/O signals with PIC	High	Low	Communication inhibited
	Low	High	Host requests to send

6.6. PS/2 Interface

To control a PS/2 mouse by connecting the data and clock lines of the PS/2 mouse to the I/O port of the PIC16F886, the PS/2 mouse and the PIC16F886 communicate by changing the output of the I/O port of the PIC16F886. Table 3 shows the basic communication specifications. When both the data and clock lines are high, the device is in the idle state, waiting for instructions from the host. When the data line is high and the clock line is low, communication is prohibited. When the data line is low and the clock line is high, the device requests an instruction from the host and begins to output a clock signal from the clock port. A software program is created and executed following steps 1 through 4 below, and we confirm communication between the PIC16F886 and the PS/2 mouse.

1. Turn on the power and set both the data and clock lines to high.
2. Set the clock line low to disable communication.
3. Set the data line low.
4. Release the clock line (wait for input), generate a clock from the PS/2 mouse and request a transfer from the PIC16F886.

6.7. Acquisition of position data in two-dimensional coordinates

After confirming communication between the PIC16F886 and the PS/2 mouse, the PIC16F886 can request data from the PS/2 mouse. The PIC16F886 sends all instructions as hexadecimal commands to the PS/2 mouse. The PS/2 mouse reads these pulses and executes the instructions. To get the necessary data from the PS/2 mouse, the PS/2 mouse has four modes: 1, 2, 3 and 4.

5. Reset Mode: Resets all mouse data values to default. This mode starts automatically when the mouse is turned on.
6. Stream mode: When the mouse detects a change in motion or a button change, it sends that data back to the host. Nearly all PS/2 mice operate in this mode. When the mouse is powered on and data reporting is enabled, this mode is automatically enabled.
7. Remote mode: It does not send any return data, even if the mouse moves, and sends data only when requested by the host. After sending the data, it starts resetting each data value in the mouse.

8. Wrap mode: The mouse sends back to the host the data bytes of the instructions it received from the host. The only exception is the command to enter reset mode. This mode is used for communication tests only. To exit this mode, the reset mode command must be sent.

The above are the modes built into a standard PS/2 mouse. In this study, we use the stream mode to measure the motion of a mobile robot. The data sent from a PS/2 mouse to the host is 3 bytes for a 3-button mouse and 4 bytes for a mouse with a scroll wheel. Table 4 shows the data stored in each byte. Yv and Xv represent the overflow (not calculable) in the Y and X directions, respectively, and Ys and Xs represent the positive and negative motion in the Y and X directions. The X-axis movement amount data is in the second byte, and the Y-axis movement amount data is in the third byte.

Tab. 4. Mouse data bite

CH(bit/bite)	7	6	5	4	3	2	1	0
1st	Yv	Xv	Ys	Xs	1	Center button	Right button	Left button
2nd	X7	X6	X5	X4	X3	X2	X1	X0
3rd	Y7	Y6	Y5	Y4	Y3	Y2	Y1	Y0
4th	0	0	Button	Button	Z3	Z2	Z1	Z0

Tab. 5. Commands for the PS/2 mouse

Bit	Command	Bit	Command	Bit	Command	Bit	Command
FF	Reset	F4	Enable data reporting	EE	Set wrap mode	E9	Status request
FE	Resend	F3	Set sample report	EC	Reset wrap mode	E8	Set resolution
F6	Set default	F2	Get device ID	EB	Read data	E7	Set scaling 2:1
F5	Disable data reporting	F0	Set remote mode	EA	Set stream mode	E6	Set scaling 1:1

The button-related bit should return a value of 1 at the moment the mouse button is pressed. However, we do not use this bit in this study. Although we use a mouse with a scroll wheel, we do not need the scroll wheel button when measuring the amount of movement. We remove some components related to the scroll wheel and buttons from the board. It allows us to read the first three bytes of the four bytes of data returned by the mouse. The PS/2 mouse receives a total of sixteen types of hexadecimal instructions from the host. Table 5 shows the instruction commands and their contents. The software developed uses only the reset command and the data reporting enable command. When data reporting is enabled, it automatically switches to stream mode. The information from the optical mouse via the PIC microcontroller can be processed using a program written in C language (CCS). Some I/O ports of the PIC microcontroller are opened and used to control the PS/2 mouse. The data in two-dimensional coordinates is obtained by switching the high and low outputs of these I/O ports and sending some commands to the optical mouse from the PIC microcontroller. The data returned from the optical mouse to the PIC microcontroller consists of a total of 4 bytes, and the necessary selected data among the returned data is processed in the calculation algorithm and considered as the amount of appropriate movement of the mobile robot in the two-dimensional coordinate. The procedure for extracting data from a PS/2 mouse is as follows: 1 to 4 below.

9. Turn on the mouse and check the clock generation.
10. Send a reset command to the mouse and initialize all the data in the mouse.
11. Allow receiving data reports and switch to stream mode.
12. Check whether the X coordinate of the mouse is positive or negative and obtain the data.
13. Check whether the Y coordinate of the mouse is positive or negative and obtain the data.
14. Divide the obtained data by the number of counts per millimeter, and convert to millimeter units. If an error occurs in steps i) to vi), the error value returns to the PIC16F886, and the operation for each step repeats.

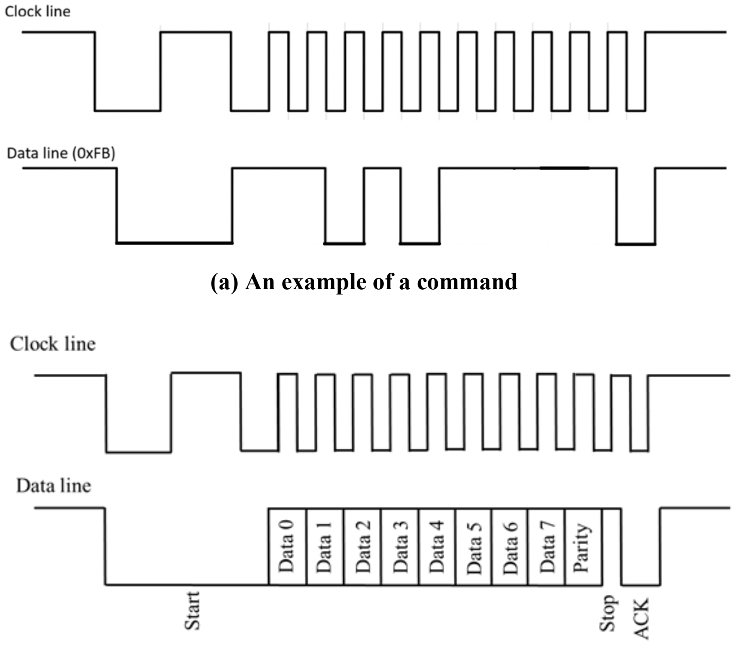

(a) An example of a command

(b) An example of reading data

Fig. 18. PS/2 communication examples

As a result of communication simulation using the created program, the response time of the optical mouse was 5 ms. According to the following steps, the motion data is in the local X-Y coordinate system of the mouse. Figure 18 shows examples of the signal processing sequence ((a) command, (b) read data).

As mentioned earlier, after the PA sensor system is turned on, the output of the gyroscope module is measured 100 times at 0.1 s intervals in a stationary state. We assume that the actual output value of the gyroscope is equal to the average of the measured values. We also consider the actual change response of the output value in the orientation of the mobile robot as the deviation from the average value. For the orientation sensor, the orientation angle data in the stationary state of the mobile robot is measured ten times at intervals of 0.15 s. Using the average value of the output and the deviation value from the average value, we estimate the rotation angle of the mobile robot. Once the initial calibration of the two sensors is completed, the program that measures the robot's motion begins. In the mobile robot, the optical sensor of the mouse outputs data whenever it detects motion. The optical sensor receives rotation angle data from the orientation sensor when the gyroscope module detects rotation of the mouse body. The linear transformation of the rotation is estimated based on the rotation angle data. After the linear transformation of the rotation of the mouse, the coordinate values of the mouse are output.

7. OPERATIONAL EXPERIMENT OF PA SENSOR SYSTEM

7.1. Data detection from the optical sensor

First, we use a program that controls only the optical mouse to verify that the optical sensor is working properly.

We move the optical mouse along a rectangular path on a horizontal plane that is 248 mm long and 185 mm wide. Figure 19 shows the values obtained from the PA sensor system. As a result, after moving the optical mouse, the error in both the X-axis and Y-axis movements was about 1 mm. The optical mouse and its optical sensor can operate with an error of 0.40 to 0.54%, which was confirmed.

7.2. Data detection from the orientation sensor

We examine the performance of the orientation sensors in terms of influence due to the surrounding environment. We install an HMC6352 orientation sensor on the omni-robot. We test the robot to rotate at a constant speed, and measure the orientation sensor output values in the room. We set the rotation speed of the robot to 1.8 rad/sec. Figure 20 shows the sensor output values when the orientation sensor is rotating. We also obtain values in time responses in the circumstances such as the center of the room, near a pillar, a wall, and an iron desk. As a result, the orientation sensor did not output any errors, and there was no significant difference in the sensor output values measured in each location.

7.3. Data detection using the PA sensor system

As Figure 11 shows the PA sensor system mounted on an electronic board. The electronic boards for controlling the PA system are located in a mobile robot with omnidirectional wheels (TDO48, manufactured by Tosa Denshi Co., Ltd.). The trajectory of the mobile robot can be estimated using the control system described above. A controller (VS-C3, Vstone Co., Ltd.) is used to operate the mobile robot. This allows the robot's trajectory data to be output from the PA sensor system. In addition, the orientation sensor is located 100 mm from the motor and at a height of 137 mm from the ground to avoid the influence of the magnetic field generated by the motors and other electronic components installed in the mobile robot.

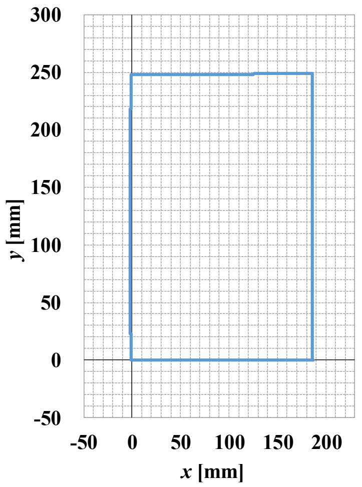

Fig. 19. The trajectory detected

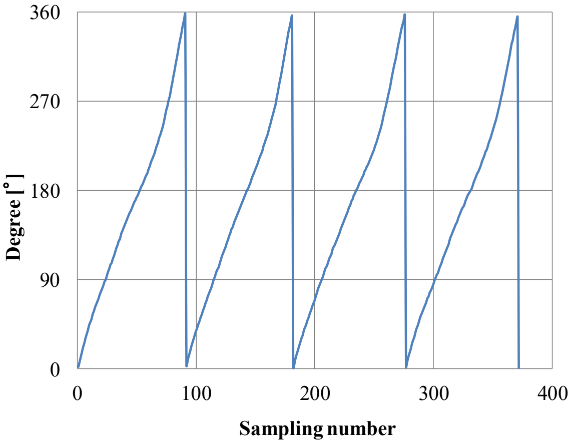

Fig. 20. The output value of the azimuth sensor by the optical sensor

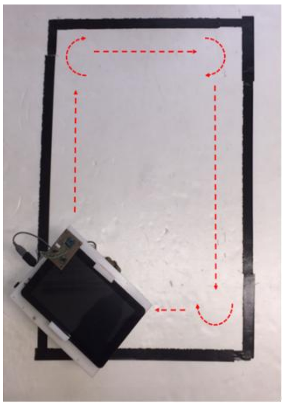

Fig. 21. The robot and the guidelines of a rectangle

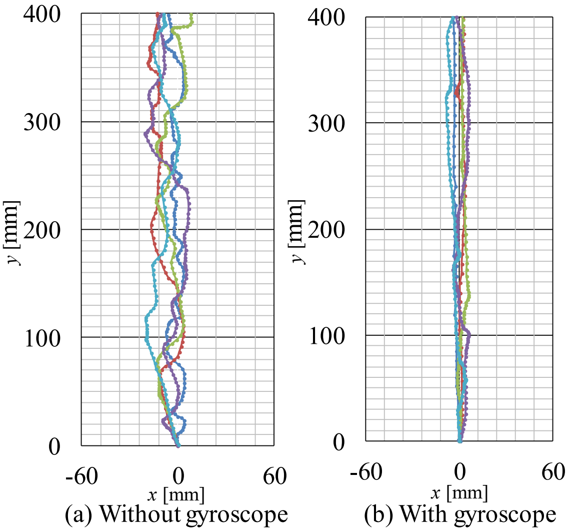

Fig. 22. The trajectory of the robot in the y-direction when the robot moves directly along the straight line

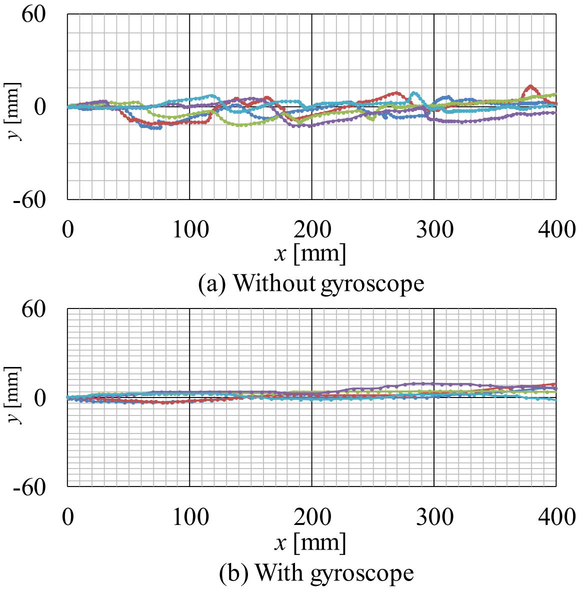

Fig. 23. The trajectory of the robot in the x-direction when the robot moves directly along the straight line

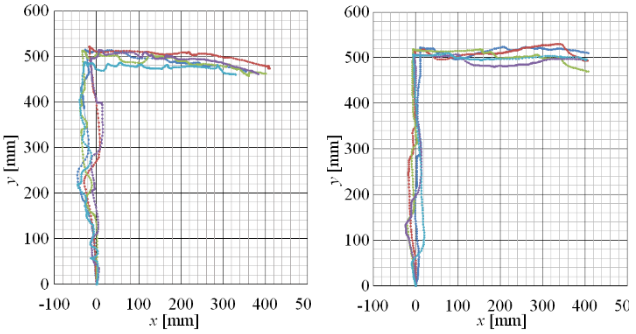

(a) Without gyroscope

(b) With gyroscope

Fig. 24 The trajectory of traverse movement of the robot at the right-angle L-shaped curve

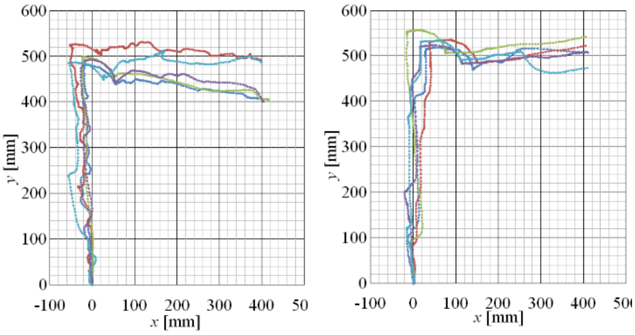

(a) Without gyroscope

(b) With gyroscope

Fig. 25 The trajectory turn movement with the change in direction of the robot at the right-angle L-shaped curve

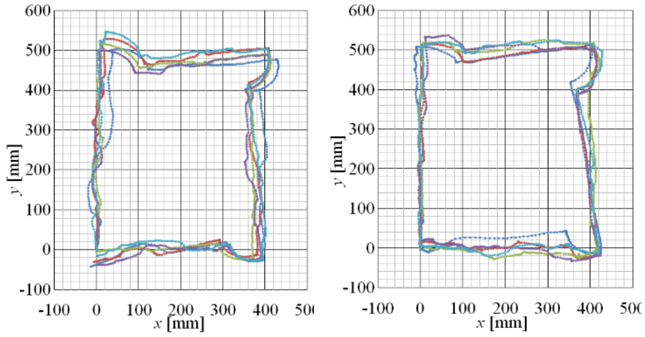

(a) Without gyroscope

(b) With gyroscope

Fig. 26. The trajectory of the rectangle curve movement with the change in direction of the robot

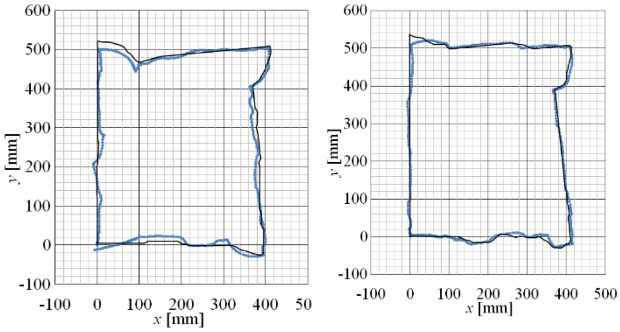

(a) Without gyroscope

(b) With gyroscope

Fig. 27. The trajectory of the rectangle movement of the robot and the marker

The electronic board of the developed PA sensor system is attached to the omnidirectional robot to obtain its motion trajectory. The trajectories of the robot are obtained both when the gyro sensor module is not operating and when it is operating. Figure 21 shows the photograph of the robot in motion.

The motion patterns of the mobile robot include forward motion, backward motion, straight motion from forward motion to the side, and rectangular motion with a change of direction. The robot repeated these patterns five times. Then the microcomputer recorded the trajectory of the mobile robot in the memory IC of the microcomputer. Figures 22 to 26 show the trajectory plots of the experiments. Each figure plots the trajectory data of the robot: (a) when using the gyroscope sensor signal, and (b) when not using the gyroscope sensor signal. We understood that the situation of data acquisition for the amount of movement indicates that the gyroscope sensor is more effective and the PA sensor system works more correctly. Thus, with a gyroscope module in the PA system, the effects of errors in the orientation sensor and the error in the amount of movement caused by vibrations in the main body of the mobile robot are reduced. A marker pen was attached to the mobile robot and the robot was moved along a surface while drawing a path. Figure 27 shows the actual measurements of the path along the surface (black solid line) and the values obtained from the PA sensor system (blue solid line) plotted on a graph.

8. CONCLUSIONS

In this paper, we developed a dead-reckoning sensor system using optical, orientation, and gyroscopic sensors to perform highly accurate self-position estimation for a mobile robot moving in indoor environments. Thus, we proposed a PA sensor system mounted on a mobile robot. Furthermore, in the experiment, the effectiveness of the sensor system in detecting the motion trajectory of the mobile robot was certified.

Conflicts of interest

The authors declare no relevant conflicts of interest regarding this work.

REFERENCES

Barbera, A., Horst, J., Schlenoff, C., Wallace, E., & Aha, D. (2003). Developing world model data specifications as metrics for sensory processing for on-road driving tasks. *Performance Metrics for Intelligent Systems, Workshop*.

Bensalem, S., Gallien, M., Ingrand, F. F., & Kahloul, I. (2008). Designing autonomous robots. *IEEE Robotics & Automation Magazine*, *16*(1), 67 – 77. https://doi.org/10.1109/MRA.2008.931631

Bui, T.-L., Tran N.-T. (2023). Navigation strategy for mobile robot based on computer vision and YOLOV5 network in the unknown environment. *Applied Computer Science*, *19*(2), 82–95. https://doi.org/10.35784/acs-2023-16

Cai, K., Chen, W., Wang, C., Zhang, H., & Meng, M. Q.-H. (2023) Curiosity-based robot navigation under uncertainty in crowded environments. *IEEE Robotics and Automation Letters*, *8*(2), 800-807. https://doi.org/10.1109/LRA.2022.3232270

Correll, N., Hayes, B., Heckman, C., & Roncone, A. (2021). *Introduction to autonomous robots: Mechanisms, sensors, actuators, and algorithms*. The MIT Press.

Czarnecka, A., Sobaszek, Ł., Świc, A. (2018). 2D image-based industrial robot end effector trajectory control algorithm. *Applied Computer Science*, *14*(1), 73–83. https://doi.org/10.23743/acs-2018-07

DeSouza, G. N., & Kak, A. C. (2002). Vision for mobile robot navigation: A Survey, *IEEE Transactions on Pattern Analysis and Machine Intelligence*, *24*(2), 237-267. https://doi.org/10.1109/34.982903

Ichihara, K., Hasegawa, T., Yuta, S., Ichikawa, H., & Naruse, Y. (2022). Waypoint-based human-tracking navigation for museum Guide robot. *Journal of Robotics and Mechatronics*, *34*(5), 1192-1204. https://doi.org/10.20965/jrm.2022.p1192

Imaoka, N., Kitazawa, K, Kamezaki, M., Sugano, S., & Ando T. (2020). Autonomous mobile robot moving through static crowd: Arm with one-DoF and hand with involute shape to maneuver human position. *Journal of Robotics and Mechatronics*, *32*(1), 59-67. https://doi.org/10.20965/jrm.2020.p0059

Kidono, K., Miura, J., & Shirai, Y. (2000). Autonomous visual navigation of a mobile robot using a human-guided experience. *Robotics and Autonomous Systems*, *40*(2-3), 121-130. https://doi.org/10.1016/S0921-8890(02)00237-3

Lewis. F. L., & Ge, S. S. (2006). *Autonomous mobile robots: Sensing, control, decision making and applications*. Routledge Taylor & Francis Group.

Morales, Y., Carballo, A., Takeuchi, E., Aburadani, A., & Tsubouchi, T. (2009). Autonomous robot navigation in outdoor cluttered pedestrian walkways. *Journal of Field Robotics*, *26*(8), 609-635. https://doi.org/10.1002/rob.20301

Patel, R., Cox, R., & Correll, N. (2018). Integrated proximity, contact and force sensing using elastomer-embedded commodity proximity sensors. *Autonomous Robots*, 42, 1443–1458. https://doi.org/10.1007/s10514-018-9751-4

Sofman, B., Lin, E., Bagnell, J. A., Cole, J., Vandapel, N., & Stentz, A. (2006). Improving robot navigation through self-supervised online learning. *Journal of Field Robotics*, *23*(11-12), 1059–1075. https://doi.org/10.1002/rob.20169

Tsunoda, Y., Nghia, L. T., Sueoka, Y., & Osuka, K. (2023). Experimental analysis of shepherding-type robot navigation utilizing sound-obstacle-interaction. *Journal of Robotics and Mechatronics*, *35*(4), 957-968. https://doi.org/10.20965/jrm.2023.p0957

Youssefian, S., Rahbar, N., & Torres-Jara, E. (2013). Contact behavior of soft spherical tactile sensors. *IEEE sensors J.*, *14*(5), 1435–1442. https://doi.org/10.1109/JSEN.2013.2296208